2024 6th International Conference on Reconfigurable Mechanisms and Robots (ReMAR)
June 24-27, 2024. Chicago, IL, USA

Vibrating Particle Robot

Richa Batra[1*], Philippe M. Wyder[1*], Pranav Jhunjhunwala[1], Quinn A. Booth[2], Aaron Xie[2], Brian G. Small[1] and Hod Lipson[1]

2024 6th International Conference on Reconfigurable Mechanisms and Robots (ReMAR) | 979-8-3503-9596-9/24/$31.00 ©2024 IEEE | DOI: 10.1109/REMAR61031.2024.10619983

***Abstract*— To overcome the limitations of traditional monolithic robots, roboticists have proposed modular robots, swarm robots, and soft robots that can adapt to their environment and be robust to single points of failure. However, due to their many degrees of freedom, they are complex and pose operational challenges. We introduce a novel particle robot comprising vibrating units encased by a rigid chain-link boundary that can act like a soft robot. Each unit, or particle, moves by adjusting the spin direction and frequency of an internal off-axis spinning mass. The particles are simple and incapable of directed locomotion, but once combined in a particle robot, they produce deterministic motion from stochastic particle interactions. This study delves into the vibrating particle mechanism, revealing how collective movement emerges from simple, individual actions. Experimental analyses across various configurations highlight how particle quantity influences movement and direction. Notably, the robot's ability to traverse tight spaces and flow around obstacles underscores its adaptability, achieved through rigid components mimicking soft-robotics principles. Our findings illuminate the potential of harnessing stochastic interactions for deterministic outcomes, advancing the field towards more adaptable and resilient robotic systems.**

I. Introduction

To date, most robots are rigid machines that execute deterministic motion to perform repetitive tasks. However, modern applications of robotics can no longer be solely addressed by fixed-structured mechanisms [1]. As robots are deployed to navigate unfamiliar and unpredictable terrain, manipulate arbitrary shapes, and safely interact with humans, traditional robots give way to alternative approaches in design, fabrication, and control [2], [3]. These approaches include soft robots, swarm robots, modular robots, and robots based on statistical mechanics.

Soft robots, for example, incorporate materials of variable stiffness and compliance into actuators and mechanisms, often mimicking biological forms [4]. It is a growing field of research, given that soft-bodied robots tend to be impact tolerant and easily deformable when interacting with other objects [5], [6]. Yet soft robots face unique challenges; due to the many degrees of freedom inherent to compliant materials, modeling and control can prove difficult [7]. Further, soft materials may be prone to failure due to fatigue and overload or when damaged by sharp objects, which can, in turn, affect their reliability during operation [8].

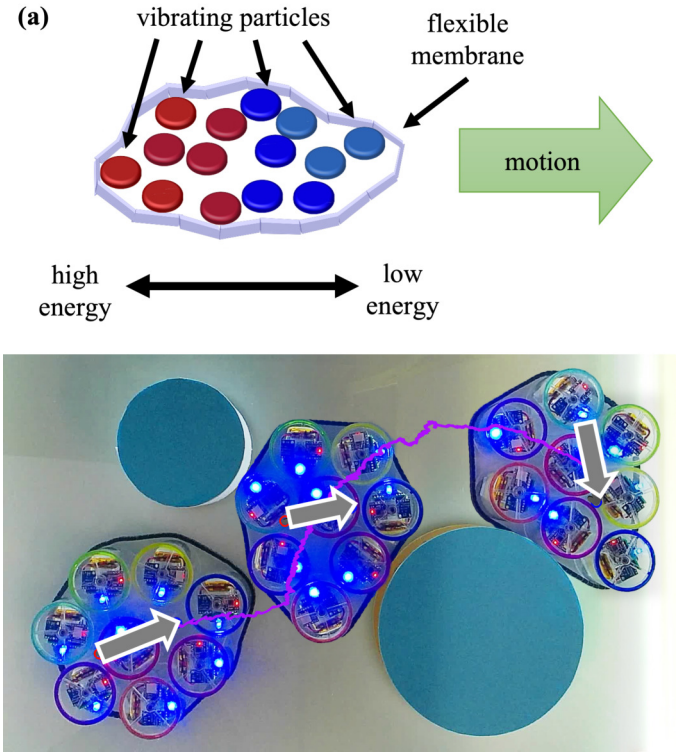


Fig. 1. Vibrating particle robot. (a) A diagram showing how deterministic motion emerges from stochastic particle interactions when an energy gradient is established by high-frequency and low-frequency vibrating particles. (b) A robot comprising 8 particles passing between two round obstacles. Half of the particles in this experiment vibrated at the maximum frequency, 6 Hz, and the other half didn't vibrate. The dotted purple line shows the vibrating particle robot's motion path, while the gray arrows show its *heading vector*, defined by the centroids of the high- and low-frequency particles.

Other bio-inspired fields include swarm and modular robots. In both cases, multiple, usually simple robots jointly perform higher-level tasks that individual units couldn't execute, but, unlike modular robots, swarm robots need to operate in a decentralized fashion [9], [10]. Some modular robots have the capacity to act in a swarm-like manner, but their focus is on combining to form larger mechanisms that can vary their topology and morphology [11], [12]. These robots are able to adapt based on the environment and objective and avoid single points of failure. The challenges with those systems lie in the complexity of the individual robot

This work was supported in part by NSF AI Institute for Dynamical Systems #2112085

[1]R. Batra, P. M. Wyder, P. Jhunjhunwala, A. Xie, B. G. Small and H. Lipson are with the Department of Mechanical Engineering, Columbia University, New York, NY 10027 USA

[2]Q. A. Booth and A. Wong are with the Department of Electrical Engineering, Columbia University, New York, NY 10027 USA

*The first two authors contributed equally to this work.

Corresponding authors richa.batra@columbia.edu and philippe.wyder@columbia.edu

Authorized licensed use limited to: Columbia University Libraries. Downloaded on November 22,2024 at 17:00:30 UTC from IEEE Xplore. Restrictions apply.

function, sensor integration, communication, and collective control.

Alternatively, robots based on statistical mechanics rely on the frequent, uncoordinated interactions between many smaller machines to produce deterministic behavior. Savoi, et al. presented a stochastic robot in which Smarticle robots collectively achieve higher-order functions when enclosed in a rigid ring, creating a Supersmarticle [13]. Their robots, comprising many two-motor flapping mechanisms, exploited statistical mechanics to achieve coordinated motion.

We first introduced the particle robotics paradigm in Li, et al., in which simple one-degree-of-freedom units, or particles, demonstrated complex behaviors when loosely coupled [14]. The particles were only capable of expanding and contracting radially. This motion was phase-modulated in response to an external signal; there was no organized coordination. Yet by allowing the particles to couple with magnets along the outer edge passively, we could exploit statistical mechanics phenomena and achieve directed motion, compliance, and robustness to failure.

We present a novel particle robot comprising vibrating particles constrained within a flexible boundary or membrane (see Fig. 1). The membrane coupling the particles is made from rigid chain links. Similar to the volumetrically oscillating particles, the vibrating particles are incapable of directed locomotion on their own. They can only vary their frequency and direction of vibration. The individual particle frequency can be set so that frequency differences between particles within the same robot produce an energy gradient across the robot. This can be done with respect to the individual particle's global position regardless of its relative position. We define this gradient with a *heading vector* pointing from the center of mass of the high-frequency/high-energy particles to the center of mass of the low-frequency/low-energy particles as depicted by the gray arrows in Fig. 1b. The vibrating particle robot functions similarly to a nonequilibrium statistical mechanics process, in which the frequency imbalance across the enclosed system drives motion from the high-energy particles toward the low-energy particles. The aggregate robot can achieve deterministic locomotion through stochastic interactions between the particles.

The vibrating particle robot mimics soft-robot behavior despite being made entirely of rigid components. Similarly to swarm and modular robots, it achieves redundancy by comprising many identical components. Each particle is so simple that it is no longer considered a robot and has the potential to be operated without centralized coordination. Compared to modular or swarm robots, particle robots' complexity of design and operation is significantly reduced.

Here, we share our study of the vibrating particle robot. First, we show the particle design used for this study. Then, we introduce our experiment environment and methods. Next, we present our findings on how the robot's behavior changes with respect to the number of particles comprising the robot and how the vibrating particle robot behaves as a soft robot in multiple experiments. Finally, we discuss our findings and share our future outlook.

II. Materials

In this section, we describe our particle robot design. This includes our discussion of hardware choices, communication, and operation. Further, we share the details of our experiment setup and video processing methods.

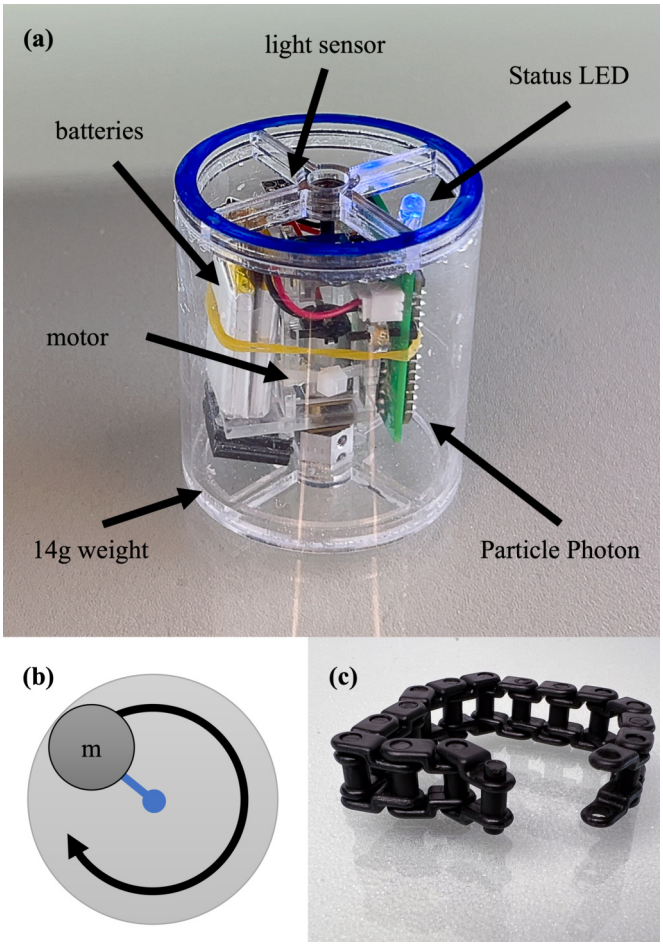


Fig. 2. Vibrating particle. (a) Closeup image of a single vibrating particle. The internal components and additional weights are arranged around the axis of rotation to form an asymmetric rotor, whose off-axis center of mass induces rotational vibration when actuated. (b) Two-dimensional schematic illustrating the physical effect of the off-axis mass created by the asymmetric rotor. (c) A plastic chain is used as the flexible membrane that encompasses the particles.

A. Vibrating Particle Robot Design

The individual vibrating particle is cylindrical, standing at 68 mm tall with a 60 mm diameter and a total weight of 263 g. Each particle contains an N20 6 Volt 300 rpm microgear DC motor powered by two 420 mAh lithium-ion polymer battery cells in series. We use a custom circuit board to connect a Particle Photon microcontroller, voltage regulator, status LED, motor driver, and light sensor (see. Fig.2a) along with the motor and batteries.

Particles achieve rotational vibration by spinning an internal off-axis mass, as depicted in the simplified diagram in Fig. 2b. We strategically arranged the electronic components, batteries, and 14 g stick-on weights around the axis of

Authorized licensed use limited to: Columbia University Libraries. Downloaded on November 22,2024 at 17:00:30 UTC from IEEE Xplore. Restrictions apply.

rotation to form an asymmetrically weighted rotor. The motor drives the rotor concentric to the outer shell via a hex-coupler.

Each particle is Wi-Fi activated and can respond to commands received through a cloud API. The particles' speed and direction of rotation can be set via API commands. We used a Python script to execute the necessary API calls for our experiments. This paper aims to demonstrate motion from stochastic particle interactions; thus, we limited ourselves to open-loop experiments.

Multiple vibrating particles must be placed inside an appropriately sized flexible boundary or membrane to form a vibrating particle robot. Our experiments used a 1/4-inch pitch plastic chain as our membrane (see Fig. 2c). It is worth noting that any lightweight and low-friction membrane of appropriate size would work if it is not elastic or adds significant damping. For example, our early tests successfully used a paper loop as a membrane. The boundary length was determined empirically, constraining the particles so they collide frequently while still allowing for the robot to deform in response to the environment.

B. Experiment Environment

The vibrating particles require a low-friction surface and are sensitive to slopes. We used a 1/2-inch thick 825 mm by 825 mm tempered glass plate as our experiment surface. The glass plate was leveled using a 3-point leveling system to avoid skewed results, and experiments were conducted in all directions to verify the setup.

The obstacles used in the round obstacle experiment shown in Fig. 1, and the rail obstacles shown in Fig. 5 were firmly mounted on the glass experiment surface using double-sided tape. The round obstacles in the experiment are 12 cm and 20 cm in diameter, and the rails are both 48 cm long, 25 mm by 25 mm cross-section aluminum extrusions. The obstacles were designed to make contact with the outside of the particle robot membrane, and not with the particles inside it.

To ensure accurate measurement of the experiment data, we placed an AprilTag in each corner of the experiment surface as a scale reference [15]. When processing our experiment data, we corrected the perspective of each video frame so it squarely aligns with the experiment surface and then tracked each particle's position individually using OpenCV's implementation of Lukežič et. al.'s Discriminative Correlation Filter Tracker with Channel and Spatial Reliability [16]. All results were computed based on the extracted position information of each particle from our experiment videos.

III. Results

This section presents our findings from characterizing the individual particles and assessing the performance of the vibrating particle robot. First, we characterize the vibration range of individual particles and highlight their limitations. Second, in section III-B, we present the effect of varying the number of particles comprising the robot on the resulting motion. Last, we assess the soft robotic behavior of the vibrating particle robot while squeezing through a narrow passage and moving around two circular obstacles.

A. Single Vibrating Particle Dynamics

Particle vibration is achieved by spinning an off-axis mass i.e., the asymmetric rotor, within the particle body to produce rotational vibration. The rotor must spin at a sufficiently high frequency for the particle body to overcome friction and start to move. If we simplify this dynamic behavior into a two-dimensional model, we can consider the force produced by the rotor as a centripetal force and assume the opposing force to be frictional. Initially, this opposing force is the static friction between the particle body and the surface. Therefore, particle vibration only begins once the rotation frequency of the rotor, ω, satisfies (1), where m_b and m_o correspond to the mass of the particle body (excluding the rotor) and the rotor mass respectively, r represents the distance between the rotor center of mass and the particle center, μ_s is the static friction coefficient and g is the gravitational constant.

$$\omega^2 > \frac{\mu_s \left(m_b + m_o\right) g}{m_o r} \tag{1}$$

On the glass experiment surface, particles overcame static friction and began to vibrate at approximately 3.5 Hz or a pulse-width modulation (PWM) motor command of ± 50. One Hertz corresponds to a rotation speed of one rotation per second. Once static friction is overcome, particle vibration can be observed.

To characterize the relationship between the motor command and single particle vibration frequency, we performed a PWM sweep on 15 different particles in both directions. For each particle, the PWM signal was set to 250, 200, 150, and 100 for 4 seconds each, then zero for 4 seconds before repeating the process in the opposite direction with inputs -250 to -100. The experiment was recorded using a 120 fps camera. We processed the video and tracked the particle position in each frame. We excluded each speed segment's first and last second to avoid capturing data from the acceleration and deceleration periods.

TABLE I
PARTICLE MOTION IN RESPONSE TO MOTOR INPUT

PWM mag	Frequency (Hz)		Amplitude (mm)	
	CCW	*CW*	*CCW*	*CW*
100	5.09 ± 0.12	5.11 ± 0.12	62.5 ± 9.1	58.1 ± 8.6
150	5.63 ± 0.14	5.61 ± 0.10	63.9 ± 6.0	62.8 ± 7.9
200	5.88 ± 0.13	5.88 ± 0.12	67.0 ± 3.6	65.7 ± 6.4
250	6.02 ± 0.15	6.00 ± 0.17	64.3 ± 11.9	64.9 ± 6.2

Table I presents the motion of the particles for PWM inputs 100, 150, 200, and 250 in both directions. The table shows the observed frequencies and amplitude with their corresponding standard deviation. When the motor input is reduced, the particle frequency reliably decreases. There is no statistically significant difference in the frequency and amplitude of the particles when rotating clockwise (CW) or

Authorized licensed use limited to: Columbia University Libraries. Downloaded on November 22,2024 at 17:00:30 UTC from IEEE Xplore. Restrictions apply.

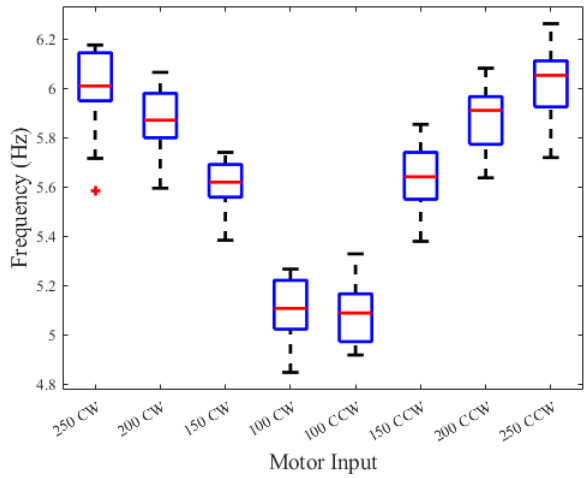


Fig. 3. Boxplot of vibration frequency given different PWM motor inputs using fully charged batteries.

counterclockwise (CCW); thus, we can trust that there is no directional bias in the design. Fig. 3 visualizes the nonlinear relationship between the PWM input and the rotational frequency.

In contrast, the vibration amplitude of the particle remains relatively stable and independent of the motor input. The vibration amplitude is a consequence of the rotor imbalance and overall weight distribution, not a function of the vibration frequency. The single-particle data shows a large variance in the vibration amplitude. We attribute this variance to the stochastic behavior of the particle primarily to drift, a common observation during the single-particle experiments.

Particle drift may be due to variable friction caused by slight imperfections on the base of the particle body and/or the experiment surface, creating temporary forces that affect the particle position. Additionally, the moment in the third dimension might be a contributing factor due to the robot's non-planar center of mass. These effects become negligible once the particles are part of a particle robot due to the much greater effect of the frequent collisions on position.

Another potential source of variance in particle behavior may be changes in the motor's operating voltage. The particle's batteries directly power the motor driver; therefore, as the battery voltage drops, so does the motor speed. To minimize this effect, the batteries were regularly replaced and charged.

B. Locomotion of the Vibrating Particle Robot at Scale

The robot's motion relies on the stochastic collisions between the particles, the boundary, and the environment. Various configurations were tested and empirically considered to achieve locomotion with the fabricated particles. We tested high- and low-frequency combinations using 6 particles, with frequencies similar to those studied in III-A (specifically with motor PWM inputs of 0, 96, 128, 192, and 255, in both directions). We observed that when low-energy particles were vibrating, the particles would intermix, and the frequency imbalance would not be maintained, resulting in random, undirected motion. Furthermore, when the high-frequency particles vibrated at approximately 5.5 Hz or less, the robots didn't experience any meaningful motion. Therefore, we chose to study the particle robot with high-energy particles set to the maximum frequency of approximately 6 Hz and the low-energy particles set to 0 Hz, maximizing the energy gradient across the robot.

Within this framework, we explored the robot's scalability and stability by varying its particle count. We tested robots with 4, 8, and 12 particles, vibrating the high-energy particles at the maximum frequency of around 6 Hz. We selected these robot sizes in order to maintain equal numbers of CW and CCW particles. An imbalance, particularly with a small number of particles, visibly biased the direction of motion and caused the robot to move in a curved path rather than a straight line due to the unbalanced torque. Fig. 4a displays the tracked trajectories of 4-, 8-, and 12-particle robots side-by-side over a 90-second period.

The experiments were conducted by setting the particle frequencies to high or low such that the *heading vector* magnitude was maximized and pointed in the desired direction of motion. The high- and low-energy particles are not mixed at the start. We varied the starting points and movement directions to offset surface bias. We ran the experiments until the robot reached the environment boundary, resulting in experiment durations of around two to five minutes.

We considered the robot's motion along its *heading vector*. The particles' stochastic behavior masks any directed robot motion in the data over short intervals. Therefore, we analyzed the robot's motion over 15-second segments sampled every 5 seconds.

Fig. 4b and c are compiled from 50 15-second segments for each configuration. The boxplot in Fig. 4b shows the projected speed of the particle robots along the initial heading vector for each time segment. The speed decreases with the increasing number of particles, as does the variance. In Fig. 4c we analyze the stability of directed motion of the particle robot. The polar histograms plot the angular change between the initial and final heading vector for each 15-second segment.

We used a circular statistics approach to test whether the direction of motion is deterministic and non-random. We performed V tests with a zero mean alternate hypothesis [17] where the zero mean signifies that the average motion is along the initial heading vector. The tests returned a consistent p-value of 0 for each configuration. While the directionality is statistically significant in all three cases, the circular histograms (Fig. 4c) show the directional variation of particle robots decreases with an increasing number of particles. Combined with the results of Fig. 4b, this shows a clear trade-off: increasing the number of particles reduces the locomotion speed but increases the directional stability of motion.

C. Soft Robotic Behavior

To test our hypothesis that vibrating particle robots can act as soft robots made from rigid parts, we designed two

Authorized licensed use limited to: Columbia University Libraries. Downloaded on November 22,2024 at 17:00:30 UTC from IEEE Xplore. Restrictions apply.

obstacle experiments that require the vibrating particle robot to deform. First, we tested if the robot could squeeze through a narrow passage. We designed an obstacle with a gradually narrowing passage that required the robot to reshape to overcome it. In addition, we included video footage of the robot squeezing through a gap in a wall-like obstacle. Second, we created an environment with two round obstacles the robot would need to navigate to reach the other side. This experiment demonstrates how the robot can deform around obstacles—similar to a gelatinous blob.

1) Squeezing through narrow passage: We created a narrow passage using two aluminum rails. We then placed a vibrating particle robot comprising 8 particles (3 vibrating clockwise, 3 vibrating counterclockwise, and 2 static ones) facing the obstacle and turned it on. The vibrating particles were spinning at 6 Hz, and the experiment was run open loop. The narrowing requires the originally 24.5 cm wide particle robot to squeeze through a gap that's 16 cm wide–35% smaller.

We found that the particle robot could deform sufficiently to squeeze through the narrow passage and move past the rails. The experiment is shown in Fig. 5. Notably, the robot automatically assumes its wider original form as soon as it clears the passage (compare frames t=85 s and t=122 s in Fig. 5). This demonstrates that the vibrating particle robot can act as a soft robot–reshaping itself in response to its environment.

The vibrating particle robot doesn't require a gradual narrowing to deform. In our video, we included an additional narrow gap experiment that shows the robot squeezing through a gap in a straight wall obstacle. The was conducted using four high-energy particles (two CW, two CCW) and four low-energy particles.

2) Adaptive motion around obstacles: We placed two round obstacles on the experimental surface: one 12cm and the other 20cm in diameter. The obstacles were placed such that the vibrating particle robot would need to deform itself to move through the passage between the two obstacles to get to the other side. The experiment used an 8-particle robot comprising 4 high-energy and 4 low-energy particles.

Fig. 1b depicts the robot's path around these obstacles, with gray arrows marking its *heading vector* and a purple line tracing its center of mass history. The supplementary video details two trials of this experiment. The first, corresponding

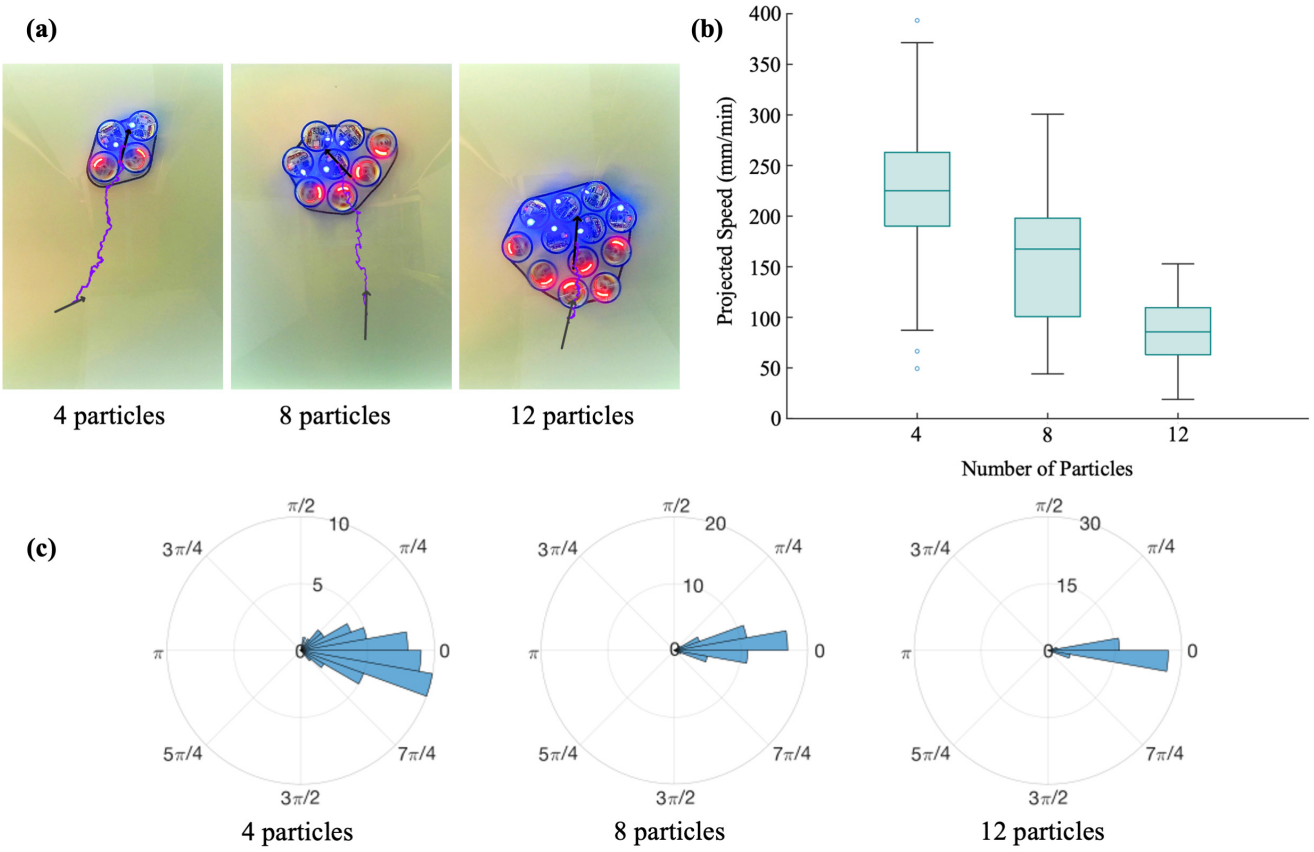


Fig. 4. Vibrating particle robots at different scales (a) From left to right, the visualized trajectory of a 4, 8, and 12 particle robot after 90 seconds. The particles glowing red vibrate at 6.0 Hz CW/CCW, while the particles in blue are not vibrating. (b) box and whisker plot of the projected speed along the heading vector over 15-second segments versus the number of particles in the vibrating particle robot. (c) From left to right, the polar histogram of the heading angle of 4, 8, and 12 vibrating particle robots over 15-second segments. The bin size is $pi/18$ radians, and the count scale (as indicated by the radius) changes in each case to better visualize the trajectory distribution. The 12-particle robot typically deviated by $\pm pi/18$ radians from its trajectory, while the 4- and 8- particle robots' directionality was more varied.

Authorized licensed use limited to: Columbia University Libraries. Downloaded on November 22,2024 at 17:00:30 UTC from IEEE Xplore. Restrictions apply.

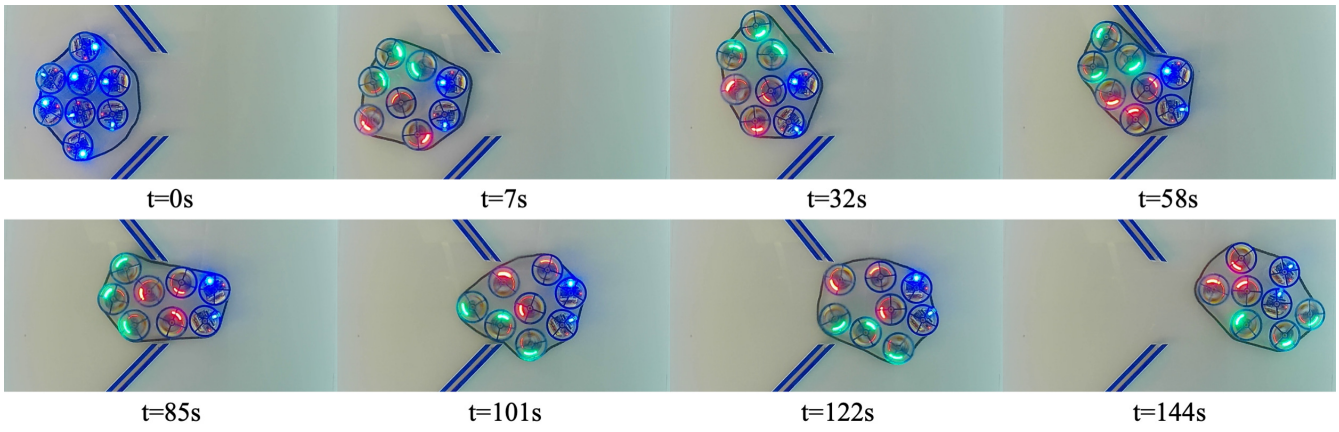


Fig. 5. Video frame sequence showing a vibrating particle robot made up of eight particles deform itself and squeeze through a narrow passage. The status LED is blue when the particle is not vibrating, red when vibrating at 6.0 Hz CCW, and green when vibrating at 6.0 Hz CW. The frames shown were selected to demonstrate the trajectory and deformation history of the robot and do not follow an even temporal spacing.

to Fig. 1b, features the robot pausing at 60-second intervals to allow the operator to adjust vibration parameters and thereby adjust the heading of the particle robot. This step proved unnecessary and was not implemented in the following experiments since the particle robot moved through the gap without additional intervention. The second showcases the 8-particle robot smoothly circumventing the round obstacles, squeezing itself through the gap without pausing. This shows the vibrating particle robot's adaptability to flow like a gelatinous blob, guided by the interaction with the obstacles. It demonstrates one way in which the system passively responds to its environment.

IV. Discussion

This work demonstrates the vibrating particle phenomena: the ability to combine stochastically vibrating, rigid components to form a soft-bodied robot capable of complex behaviors. We detailed the particle design, analyzed its performance, and provided an understanding of the design considerations. The particle robot size study demonstrated the ability to scale the robot and produce more reliable motion at the cost of speed. Lastly, we demonstrated the particle robot's compliant behavior and deformation while moving between obstacles in the environment.

In future work, we plan to explore the locomotion of the vibrating particle robot with decentralized control using the integrated light sensors. The particle vibration will solely be determined by environmental signals, ensuring particles need no individual identity or means of direct coordination. We, therefore, remove any single point of failure.

We also intend to simulate the vibrating particle robots. This will allow us to observe the particle robot with hundreds or thousands of particles. It will also enable us to systematically explore design parameters (e.g., vibration frequency and amplitude, off-axis mass to particle body mass ratio) at varying scales and sizes. In addition, we will study different control schemes.

The complexity of nature's creatures is based on basic building blocks: cells. Analogously, the vibrating particle robot could be perceived as a rough mechanical approximation of a multinucleated giant cell: the flexible membrane mimicking the cell membrane and the particles acting as cell nuclei[18], [19]. By implementing particle-to-particle communications and environmental sensors, the robot has the potential to be responsive and adaptive to its environment, mimicking complex biological systems. The vibrating particle robot provides a strong platform to study distributed and decentralized controls.

Finally, we believe designing, simulating, and studying vibrating particle robots in three dimensions is the next big challenge in particle robotics. This will likely require new forms of coupling between particles and multiple vibrating robot cells, mimicking cell wall adhesion. We envision a future where resilient and soft robots can be created at scale by combining particle robotics research with micro-electrical mechanical systems manufacturing advances.

Acknowledgment

Thanks to Denise Wong, Stephane Constantin, Adrian Wong, and Sarah Bates for contributing to the initial prototype.

References

[1] E. Garcia, M. A. Jimenez, P. G. De Santos, and M. Armada, "The evolution of robotics research," *IEEE Robotics and Automation Magazine*, vol. 14, no. 1, pp. 90–103, 2007.

[2] P. E. Dupont, B. J. Nelson, M. Goldfarb, B. Hannaford, A. Menciassi, M. K. O'Malley, N. Simaan, P. Valdastri, and G. Z. Yang, "A decade retrospective of medical robotics research from 2010 to 2020," *Science Robotics*, vol. 6, no. 60, 2021.

[3] T. B. Sheridan, "A review of recent research in social robotics," *Current Opinion in Psychology*, vol. 36, pp. 7–12, dec 2020.

[4] S. Kim, C. Laschi, and B. Trimmer, "Soft robotics: a bioinspired evolution in robotics," *Trends in Biotechnology*, vol. 31, pp. 287–294, may 2013.

[5] B. Jumet, M. D. Bell, V. Sanchez, and D. J. Preston, "A data-driven review of soft robotics," *Advanced Intelligent Systems*, vol. 4, 2022.

[6] J. Walker, T. Zidek, C. Harbel, S. Yoon, F. S. Strickland, S. Kumar, and M. Shin, "Soft robotics: A review of recent developments of pneumatic soft actuators," *Actuators*, vol. 9, 2020.

[7] D. Rus and M. T. Tolley, "Design, fabrication and control of soft robots," *Nature*, vol. 521, pp. 467–475, May 2015.

Authorized licensed use limited to: Columbia University Libraries. Downloaded on November 22,2024 at 17:00:30 UTC from IEEE Xplore. Restrictions apply.

[8] S. Terryn, J. Langenbach, E. Roels, J. Brancart, C. Bakkali-Hassani, Q. A. Poutrel, A. Georgopoulou, T. G. Thuruthel, A. Safaei, P. Ferrentino, T. Sebastian, S. Norvez, F. Iida, A. W. Bosman, F. Tournilhac, F. Clemens, G. V. Assche, and B. Vanderborght, "A review on self-healing polymers for soft robotics," *Materials Today*, vol. 47, pp. 187–205, 7 2021.

[9] A. R. Cheraghi, S. Shahzad, and K. Graffi, "Past, present, and future of swarm robotics," *Lecture Notes in Networks and Systems*, vol. 296, pp. 190–233, 2022.

[10] P. G. F. Dias, M. C. Silva, G. P. R. Filho, P. A. Vargas, L. P. Cota, and G. Pessin, "Swarm robotics: A perspective on the latest reviewed concepts and applications," *Sensors 2021, Vol. 21, Page 2062*, vol. 21, p. 2062, 3 2021.

[11] C. Zhang, P. Zhu, Y. Lin, Z. Jiao, and J. Zou, "Modular Soft Robotics: Modular Units, Connection Mechanisms, and Applications," *Advanced Intelligent Systems*, vol. 2, no. 6, 2020.

[12] J. Seo, J. Paik, and M. Yim, "Modular Reconfigurable Robotics," *Annual Review of Control, Robotics, and Autonomous Systems*, vol. 2, pp. 63–88, 2019.

[13] W. Savoie, T. A. Berrueta, Z. Jackson, A. Pervan, R. Warkentin, S. Li, T. D. Murphey, K. Wiesenfeld, and D. I. Goldman, "A robot made of robots: Emergent transport and control of a smarticle ensemble," *Science robotics*, vol. 4, 2019.

[14] S. Li, R. Batra, D. Brown, H. D. Chang, N. Ranganathan, C. Hoberman, D. Rus, and H. Lipson, "Particle robotics based on statistical mechanics of loosely coupled components," *Nature 2019 567:7748*, vol. 567, pp. 361–365, 3 2019.

[15] E. Olson, "Apriltag: A robust and flexible visual fiducial system," *Proceedings - IEEE International Conference on Robotics and Automation*, pp. 3400–3407, 2011.

[16] A. Lukežič, T. Vojíř, L. Čehovin Zajc, J. Matas, and M. Kristan, "Discriminative correlation filter tracker with channel and spatial reliability," *International Journal of Computer Vision*, vol. 126, pp. 671–688, 2018.

[17] P. Berens, "CircStat: AMATLABToolbox for circular statistics," *J. Stat. Softw.*, vol. 31, no. 10, 2009.

[18] K. Ahmadzadeh, M. Vanoppen, C. D. Rose, P. Matthys, and C. H. Wouters, "Multinucleated giant cells: Current insights in phenotype, biological activities, and mechanism of formation," *Frontiers in Cell and Developmental Biology*, vol. 10, 4 2022.

[19] T. C. Day, P. Márquez-Zacarías, P. Bravo, A. R. Pokhrel, K. A. MacGillivray, W. C. Ratcliff, and P. J. Yunker, "Varied solutions to multicellularity: The biophysical and evolutionary consequences of diverse intercellular bonds," *Biophysics Reviews*, vol. 3, p. 021305, 6 2022.

Authorized licensed use limited to: Columbia University Libraries. Downloaded on November 22,2024 at 17:00:30 UTC from IEEE Xplore. Restrictions apply.